

Understanding the anomalous $1/t^3$ time dependence of velocity correlation function in one dimensional Lennard-Jones systems

Goundla Srinivas and Biman Bagchi^{a),b)}

Solid State and Structural Chemistry Unit, Indian Institute of Science, Bangalore 560 012, India

One dimensional Lennard-Jones fluids are known to exhibit an interesting $1/t^3$ time (t) dependence of the velocity correlation function. The origin of this decay is apparently not well understood. We have studied this problem both by molecular dynamic simulations and by mode coupling theory. We find that this t^{-3} decay of the velocity autocorrelation function (VACF) arises from the coupling of the tagged particle's motion to the longitudinal current mode of the fluid. Interestingly such a decay is intern rendered possible by the Gaussian time dependence of the coherent dynamic structure factor at the relevant times. This is confirmed by the simulations of Lennard-Jones rods. The t^{-3} dependence is found to be dominant at low and intermediate densities. We show that the mode coupling theory provides an accurate description of the VACF both at short and long time limits.

I. INTRODUCTION

The diffusion coefficient of a tagged molecule shows strong dependence on the dimensionality of the system. While it exists in three and one dimensions, it diverges in the intermediate two dimensions.^{1,2} There is, however, no difficulty in defining a diffusion coefficient in arbitrary dimensions and any of the following two definitions suffice:

$$D = \lim_{t \rightarrow \infty} \frac{1}{2dt} \langle \Delta \mathbf{r}^2(t) \rangle \quad (1)$$

and

$$D = \frac{1}{d} \int_0^{\infty} dt \langle V(0) V(t) \rangle, \quad (2)$$

where $\langle \Delta \mathbf{r}^2(t) \rangle$ is the mean square displacement of a tagged particle, $V(t)$ is the velocity at time t , and d is the dimensionality of the system. The reason for the divergence of diffusion coefficient in two dimensions (2D) can be understood in terms of a long time tail in the decay of velocity time correlation function, of the form $t^{-d/2}$ (for two and three dimensions). This long time tail arises from the coupling of the tagged particle's motion with transverse current flow of the liquid. This gives rise to a logarithmic divergence of the mean-square displacement in 2D.³

No such divergence exists for three dimensions. There is a long time tail in this case also but its contribution to the diffusion coefficient is negligible. Thus, one is interested to know what happens in one dimensional systems at high density. One does not expect a divergence here because of the nonexistence of the transverse current mode and the decay of longitudinal current mode (related to the dynamic structure factor by a trivial differentiation) is sufficiently fast to pre-

clude the existence of any “dangerous” long time tail. Actually, Jepsen⁴ was the first to derive the closed form expression for the velocity autocorrelation function (VACF) and the diffusion coefficient for *hard rods*. His study showed for the first time, that the *long time* VACF decays as t^{-3} , in contrast to the $t^{-d/2}$ dependence reported for the two and three dimensions. Lebowitz and Percus⁵ studied the short time behavior of VACF and made an exponential approximation for VACF, i.e., $C_v(t) = \exp(-2t)$, for the *short times*. Haus and Raveche⁶ carried out the extensive molecular dynamic simulations to study relaxation of an initially ordered array in one dimension. This study also investigated the $1/t^3$ behavior of VACF. However, none of the above studies provides a *physical explanation* of the $1/t^3$ dependence of VACF at long times, of the type that exists for two and three dimensions.

Unlike for hard rods, no analytical solution exists for 1D LJ rods. Molecular dynamics (MD) simulations have revealed a $1/t^3$ behavior in this system also. The computer simulations of Bishop and Berne^{7,8} seem to suggest that there exists no hydrodynamic mode in one dimensional fluids. What is meant by the nonexistence of hydrodynamic mode is that there is no long lived collective excitation. In the one dimensional dense liquids, there is a well-defined cage formed around each molecule by its nearest neighbors (see Fig. 1). The relaxation of density and hence the form of the relaxation function for the dynamic structure factor (DSF) is, therefore, similar to the relaxation in a harmonic oscillator. The average frequency of the oscillator is given by the Einstein frequency. At high density, the value of this frequency is large. So the relaxation at short times is in the underdamped limit of momentum relaxation. In three dimensional liquids, the decay of the DSF at small wave number and long times is usually exponential. While an exponential-like decay eventually sets in for one dimensional fluids for small wave number relaxation also, this occurs at times much longer than in 3D. For times relevant for the decay of the

^{a)}Electronic mail: bbagchi@sscu.iisc.ernet.in

^{b)}Also at the Jawaharlal Nehru Center for Advanced Scientific Research, Jakkur, Bangalore.

velocity correlation function, DSF is a Gaussian function of time.

Another interesting question pertains to the fact that one expects a very small diffusion coefficient for a one dimensional system with harsh short-range repulsive potential, as in the case of Lennard-Jones fluid. In 3D the contribution of longitudinal current mode to diffusion is entirely negligible, while the transverse current mode contributes 5–10% at high densities.⁹ In 1D there is only the longitudinal current mode. Thus it is highly interesting to study the role of this mode.

Note that the study of diffusion in the one dimensional system is not purely academic. There are evidences of one dimensional diffusion in many biological systems, such as a long DNAs and in the case of metal surface catalytic reactions.

In this paper, we present a detailed study of diffusion in one dimensional Lennard-Jones fluid by using mode coupling theory (MCT) and MD simulations with an aim at understanding the slow decay of velocity correlation functions at long times and also the density dependence of the diffusion coefficient. We have performed a fully self-consistent mode coupling theory calculation to obtain both the short and long time behavior of $C_v(t)$. We show that MCT provides a simple interpretation of the $1/t^3$ decay of the velocity correlation function in the long time in terms of the coupling of the tagged particle's motion to the longitudinal current mode of the surrounding fluid.

The organization of the rest of the paper is as follows. In Sec. II we present the simulation details of the system under study. The detailed approach of MCT in the one-dimensional case has been described in Sec. III. Demonstration of t^{-3} decay of VACF by mode coupling theory is given in Sec. IV. Section V includes the discussion and comparison of the results obtained both by the mode coupling theory and MD simulations. We close the paper with a few conclusions in Sec. VI.

II. SYSTEM AND SIMULATION DETAILS

Our model one dimensional simulation system consists of 1000 Lennard-Jones (LJ) rods placed in a row by applying the periodic boundary conditions in one dimension. Initial velocities have been chosen from the Maxwellian velocity distribution. The rods with the assigned velocities are then allowed to interact through the pairwise additive Lennard-Jones potential, given by

$$V_{ij}(x) = 4\epsilon \left[\left(\frac{l}{x}\right)^{12} - \left(\frac{l}{x}\right)^6 \right], \quad (3)$$

where i and j represents two different LJ rods, l is the length of LJ rod and ϵ is the well depth of the interaction potential. In all the simulations mass (m) of the rods scaled to unity. The reduced parameters being used in simulations for the length, time, temperature and the density are $x^* = x/l$, $\tau = \sqrt{(m/\epsilon)}l$, $T^* = k_B T/\epsilon$, and $\rho^* = \rho l$, respectively. The time dependent diffusion $D(t)$ is scaled by l^2/τ .

We have studied a wide range of densities starting from a lower density $\rho^* = 0.1$ to a maximum of $\rho^* = 0.9$ at a reduced temperature $T^* = 1.0$. Length of the simulation box

has been adjusted from run to run to obtain the required density. This system behaves exactly like the point atoms placed at a distance of $1/\rho$ interacting in a volume of $V = L - Nl$, where L is the length of the simulation box and N , the number of LJ rods. Our simulations were carried out at constant volume and energy (microcanonical ensemble). The Newtonian equations of motion were numerically solved by using the Verlet algorithm with a time step equal to 0.0005τ at all the densities except in the case of very low density ($\rho^* = 0.1$), where we had to use a larger timestep, $\Delta t = 0.002\tau$. The cutoff range of the interaction potential was 6.0σ , which is sufficient enough to ensure the short range interactions in one dimension. In all the cases, the system has been equilibrated up to 50 000 timesteps. Simulation runs have been carried out for another 100 000 production time steps after the equilibration, during which the velocities and the positions of the rods have been stored at each 10th step for subsequent analysis. Such simulation runs were repeated three times with different initial velocity distribution. The required quantities has been calculated by averaging over all the runs.

III. MODE COUPLING THEORY ANALYSIS

We have carried out the self-consistent mode coupling theory study to understand the origin of the slow t^{-3} decay of VACF and also to calculate the time dependent diffusion in one dimension. In order to calculate either VACF or diffusion coefficients, we need the two particle direct correlation function, $c(x)$, and the radial distribution function, $g(x)$. Here x denotes the separation between the centers of two LJ rods. In order to make the calculations robust we have used the $g(x)$ obtained from simulations. The frequency (z) dependent velocity correlation function $C_v(z)$ is related to the frequency dependent friction by the following generalized Einstein relation,

$$C_v(z) = \frac{k_B T}{m(z + \zeta(z))}, \quad (4)$$

where $\zeta(z)$ is the frequency dependent friction.

In mode coupling theory the full friction is decomposed into a short and a long time part. Short time part arises from the binary collisions of tagged particle with the surrounding solvents and the long time part originates from the correlated recollisions. Final expression for the frequency dependent friction used to calculate both VACF and time dependent diffusion is given by¹⁰

$$\zeta(z) = \zeta^B(z) + \zeta^R(z), \quad (5)$$

where $\zeta^B(z)$ is the binary part of the zero frequency friction, $\zeta^R(z)$ is the ring collision term, which contains the contributions from the repeated collisions to the total friction. In 1D we can replace the ring collision term in the above expression by

$$\zeta^R(z) = R_{\rho\rho}(z) + 2\zeta^B(z)R_{\rho l}(z) + \zeta^B(z)R_{ll}(z)\zeta^B(z). \quad (6)$$

The above expression is similar to that of 3D^{10,9} but with the absence of the term that contains the contribution from transverse current to the total friction. In the above expression $R_{\rho\rho}(z)$ contains the coupling to the density and is given by

$$R_{\rho\rho}(t) = \frac{\rho k_B T}{m} \int [dq'/(2\pi)] q'^2 [c(q')]^2 \times [F^s(q',t) - F_0^s(q',t)] F(q',t), \quad (7)$$

$c(q)$ is the Fourier transform of $c(x)$. $R_{ll}(z)$ contains the longitudinal current while $R_{\rho l}$ includes the coupling of density and longitudinal current, which can be expressed by the following expressions in one dimension by following the similar procedure used in 3D,^{10,11} and

$$R_{ll}(t) = -\frac{1}{\rho} \int [dq'/(2\pi)] \times [\gamma_d^l(q') + (\rho q^2/m\beta) c(q')]^2 \omega_0^{-4} \times [F^s(q',t) - F^0(q',t)] C_l(q',t) \quad (8)$$

and

$$R_{\rho l}(t) = - \int [dq'/(2\pi)] c(q') \times [\gamma_d^l(q) + (\rho q^2/m\beta) c(q')] \omega_0^{-2} \times [F^s(q',t) - F^0(q',t)] \frac{d}{dt} F(q',t), \quad (9)$$

where $\gamma_d^l(q)$ is the distinct part of the second moment of the longitudinal current correlation function, which is given by the following equation:

$$\gamma_d^l(q) = -\frac{\rho}{m} \int dx \cos(qx) g(x) \frac{d^2}{dx^2} v(x) \quad (10)$$

and ω_0 is the well-known Einstein frequency in 1D and is given by

$$\omega_0^2 = \frac{\rho}{m} \int dx g(x) \frac{d^2}{dx^2} v(x). \quad (11)$$

$\zeta^B(t)$ is the binary part of the friction whose expression is given by

$$\zeta^B(t) = \omega_0^2 \exp(-t^2/\tau_\zeta^2). \quad (12)$$

The relaxation time τ_ζ is determined from the second derivative of the above expression for $\zeta^B(t)$, which is given by the following equation,

$$\frac{\omega_0^2}{\tau_\zeta^2} = \frac{\rho}{3m^2} \int dx \frac{d^2}{dx^2} v(x) g(x) \frac{d^2}{dx^2} v(x) + \frac{1}{4\pi\rho} \int dq \gamma_d^l(q) (S(q) - 1) \gamma_d^l(q) \quad (13)$$

the static structure factor, $S(q)$, appearing in the above expression is calculated by using the one-dimensional Fourier transform of the radial distribution function. The Fourier transformed two particle direct correlation function $c(q)$ is obtained through the well-known Ornstein-Zernike relation.¹²

Calculational procedure of all the dynamical variables appearing in the above expressions namely the dynamic structure factor, $F(q,t)$ and its inertial part $F_0(q,t)$, the self-dynamic structure factor $F^s(q,t)$, and the inertial part of the

same $F_0^s(q,t)$ can be found in detail elsewhere.¹¹ We skip the calculational details of all the above quantities, simply because the expressions for these quantities remains the same except for the terms that include the dimensionality.

The self-consistent iterative scheme has been applied for the calculation of $F^s(q,t)$ in the following fashion. The full friction appearing in $C_v(z)$ expression [Eq. (4)] is initially replaced by its binary part, $\zeta^B(z)$ as a first approximation. Resulting $C_v(z)$ is Laplace inverted to get $C_v(t)$ which is then used in the following expression to get mean square displacement:

$$\langle \Delta x^2(t) \rangle = 2 \int_0^t C_v(\tau) (t - \tau) d\tau \quad (14)$$

the MSD so obtained is used as input in the following self-dynamic structure factor expression

$$F^s(q,t) = \exp\left(-\frac{q^2 \langle \Delta x^2(t) \rangle}{2}\right), \quad (15)$$

which essentially is used to calculate $R_{\rho\rho}(t), R_{ll}(t)$ and thus $\zeta(t)$. The resulting total friction is used to calculate new $C_v(t)$, which again is used to determine MSD and thus $\zeta(t)$. The above iterative scheme has been continued until the $C_v(t)$ obtained from two consecutive steps completely overlaps. The above scheme provides a $C_v(t)$ fully consistent with the frequency dependent friction.¹³

The longitudinal current correlation function, $C_l(q,t)$, is related to the dynamic structure factor by the following expression:

$$C_l(q,t) = -\frac{m^2}{q^2} \frac{d^2}{dt^2} F(q,t). \quad (16)$$

It is important to note that at sufficiently long times the only significant contribution to the integral of Eq. (8) arises from small wave numbers. Note that the only existing current mode is the longitudinal one and is directly related to the $F(q,t)$ through the above equation.

IV. LONG TIME BEHAVIOR OF VACF

It can be shown from Eqs. (4)–(8), that the long time behavior of VACF is determined by the longitudinal current term $R_{ll}(t)$. This also follows from simple but elegant treatment of Gaskell and Miller who considered the coupling of the tagged particle velocity with current modes of the liquid.⁹ The expression of $R_{ll}(t)$ is given by Eq. (8).

In the limit of small q (long wavelength) the following limiting condition holds:

$$\frac{[\gamma_d^l(q') + (\rho q^2/m\beta) c(q')]}{\omega^4} \xrightarrow{q \rightarrow 0} 1. \quad (17)$$

Thus, at the long times, the time dependence of $C_v(t)$ and hence $R_{ll}(t)$ can be expressed as

$$C_v(t) \approx R_{ll}(t) \sim \int dq' F^s(q',t) C_l(q',t). \quad (18)$$

The long time behavior of the integrand in the above equation is determined by $C_l(q,t)$. Now $C_l(q,t)$ is determined by

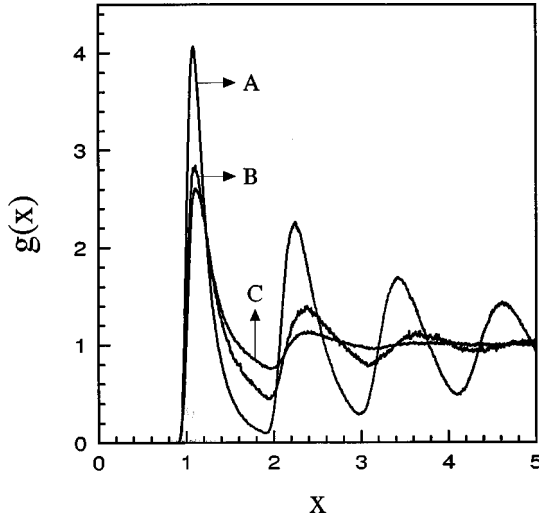


FIG. 1. The simulated two particle radial distribution function, $g(x)$ is plotted against the separation of the rods at various densities at $T^*=1.0$. Rapid disappearance of the second and higher solvation shells with decreasing density is clearly evident from the figure. The lines marked by *A*, *B*, and *C* correspond to the densities $\rho^*=0.82$, 0.6, and 0.3, respectively.

the intermediate scattering function as given by Eq. (16). When Eq. (16) is substituted in the above equation, we get

$$R_{ll}(t) \approx \int dq \frac{d^2}{dt^2} F(q,t). \quad (19)$$

The important point now to note is that in 1D hard rods, $F(q,t)$ decays mostly as a Gaussian function of time. At small q decay, $F(q,t)$ can be given as

$$F(q,t) \approx \exp(-aq^2t^2), \quad (20)$$

where a is a constant.

As already mentioned, the Gaussian decay of $F(q,t)$ at small wave numbers at large density is a manifestation of the well-defined cage around each molecule. Thus, the relaxation of density remains nearly elastic for sufficiently long times. It is further assumed that on the time scale of decay of $F(q,t)$, the relaxation of the self-term, $F_s(q,t)$ is negligible. By making this Gaussian ansatz for $F(q,t)$ and substituting $C_l(q,t)$ in Eq. (8), we get the following expression for the longitudinal current:

$$R_{ll}(t) \approx \frac{m^2}{2\sqrt{\pi}\rho t^3}, \quad (21)$$

which simply shows that in the long times longitudinal current goes as t^{-3} .

Note that the two essential ingredients of the above derivation is the contribution of the longitudinal current term and the Gaussian decay of the intermediate scattering function. The above derivation is by no means rigorous, but numerical calculations verify both the above reasons as the origin of t^{-3} time dependence of VACF. As demonstrated later $F(q,t)$ decays as Gaussian (in time) at small q .

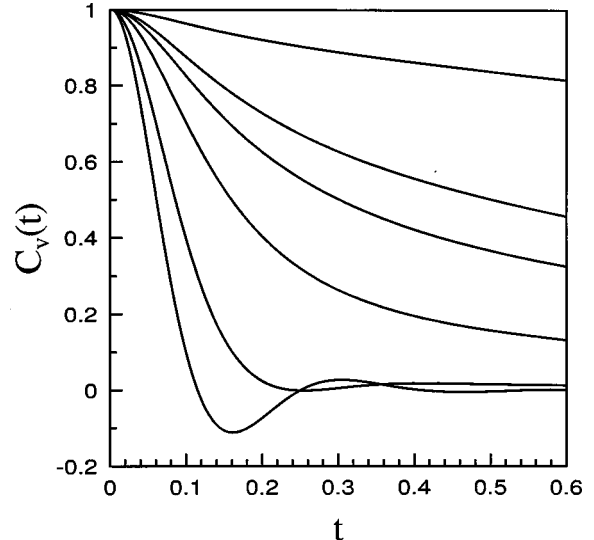


FIG. 2. Normalized VACF obtained from simulations is plotted against the reduced time at various densities at $T^*=1.0$. The lines from top to bottom represent the case with $\rho^*=0.1$, 0.3, 0.4, 0.6, 0.82, and 0.9, respectively.

V. RESULTS AND DISCUSSION

As explained earlier the structure of one dimensional system changes drastically even for the mild changes in density. In Fig. 1, we have plotted the simulated radial distribution function $g(x)$ at various densities to show the effect of changes in density on the structure of the 1D fluid.

Figure 2 shows the effect of density on VACF in 1D. All the features observed in the figure can be explained in terms of the local structure. At high density there exists a negative region in VACF, which arises due to the ‘‘backscattering.’’ Apart from the high density case, at intermediate and low densities, the pronounced slow long time decay of VACF has been observed. It is difficult either to study or to

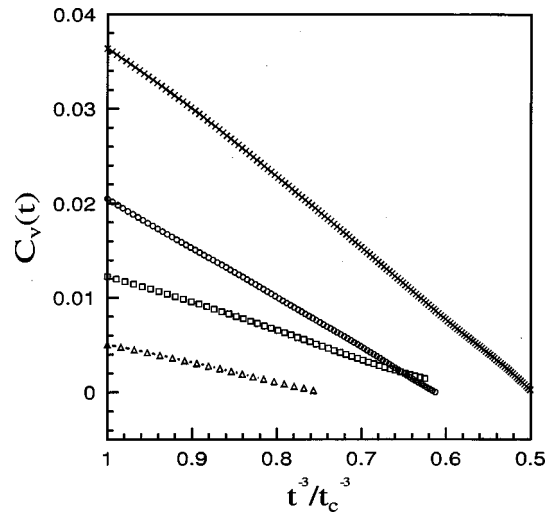


FIG. 3. The long time tails of $C_v(t)$ obtained from simulations are plotted against $(t_c/t)^3$ at various densities at $T^*=1.0$. t is the reduced time and t_c is the time at which the long time tail of $C_v(t)$ started approaching zero. The different symbols from top to bottom represent the $C_v(t)$ at reduced densities 0.3, 0.4, 0.6, and 0.82, respectively. The figure shows the dominance of t^{-3} decay in $C_v(t)$ at low and intermediate densities.

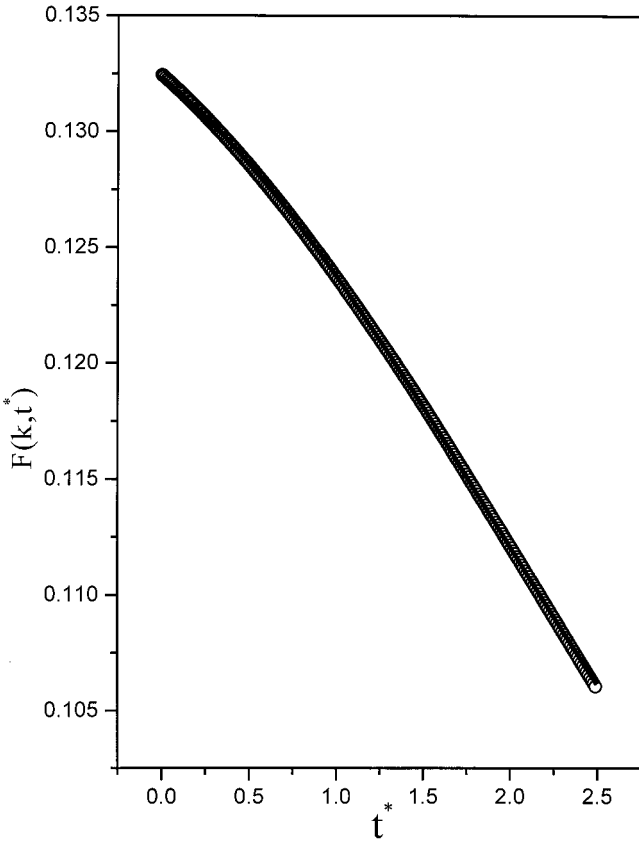


FIG. 4. The intermediate scattering function, $F(q,t)$, obtained from simulations, is plotted against the time at an intermediate density $\rho^*=0.6$ and $T^*=1.0$ at a low wave vector value of $ql=0.1206$. Symbols show the simulation results and the full line is the Gaussian fit. This figure clearly demonstrates the Gaussian behavior of $F(q,t)$ in the $q\rightarrow 0$ limit.

extract the interesting information from the long time tail of $C_v(t)$ at high densities due to the presence of both the negative region and the huge oscillations. To overcome this difficulty we have studied a wide range of densities.

In Fig. 3 the long time tail of VACF is plotted after an initial decay. This figure clearly shows the t^{-3} behavior of $C_v(t)$ in the long time over a wide range of densities. This decay is more dominant, at low and intermediate densities. This can be attributed to the disappearance of local structure and the existence of positive tail in $C_v(t)$ over a longer time. On the other hand, the existence of long time tail will be suppressed at higher densities due to the presence of the negative region and the oscillations over a longer time which masks the $1/t^3$ decay of VACF in the long time.

In Fig. 4, the normalized dynamic structure factor $F(q,t)/S(q)$ is plotted at a small wave vector value, $ql=0.1206$, in the time domain where the VACF shows pronounced t^{-3} decay. Circles show the simulated values and the full line is the Gaussian fit. As seen from the figure, $F(q,t)$ is a Gaussian function of time in the $q\rightarrow 0$ limit. This is an important observation since it provides the key to the physical origin for the slow decay of $C_v(t)$.

Time dependent diffusion ($D(t)$) shows the approach to long time diffusion. $D(t)$ can be expressed as

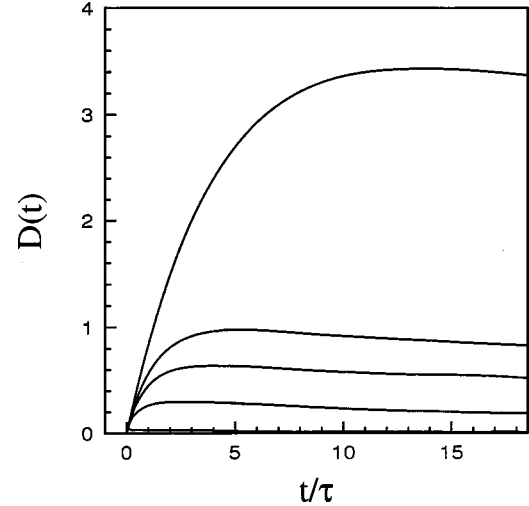


FIG. 5. The time dependent diffusion ($D(t)$) obtained from the simulated $C_v(t)$ is plotted against the reduced time at various densities at $T^*=1.0$. The curves from top to bottom represent the $D(t)$ for the different densities, namely $\rho^*=0.1, 0.3, 0.4, 0.6$, and 0.82 .

$$D(t) = \frac{k_B T}{m} \int_0^t C_v(\tau) d\tau. \quad (22)$$

The result, the density dependence of time dependent diffusion in 1D, is shown in Fig. 5. This figure clearly shows the existence of the diffusion coefficient in 1D. Even at high densities there exists a small but nonvanishing diffusion coefficient.

Normalized VACF obtained from self-consistent mode coupling theory has been plotted in Fig. 6, against the time at a medium density $\rho^*=0.6$ and $T^*=1.0$. Here, we have compared the simulated $C_v(t)$ with the $C_v(t)$ obtained from MCT. In Fig. 7, we compared the $C_v(t)$'s at a lower density $\rho^*=0.4$. Similar results have been obtained at other densi-

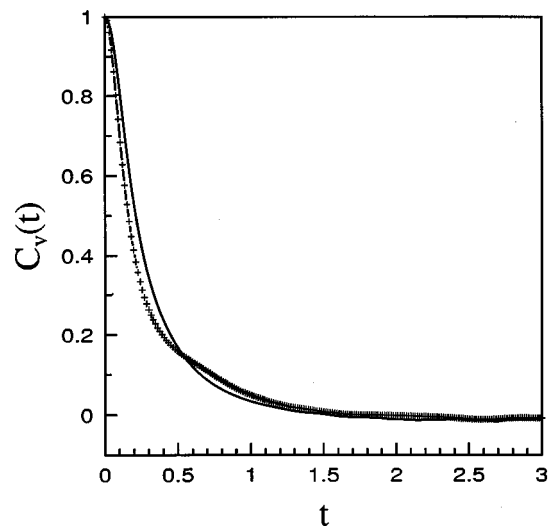


FIG. 6. $C_v(t)$ obtained from the MCT and from the MD simulations have been plotted against the reduced time at $\rho^*=0.6$ and $T^*=1.0$. Symbols show the simulated $C_v(t)$ and the full line represents the $C_v(t)$ obtained by MCT.

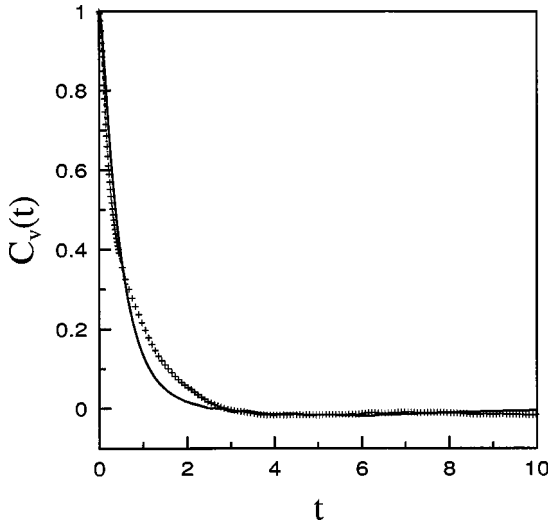


FIG. 7. $C_v(t)$ obtained from the MCT and from the MD simulations have been plotted against the reduced time at $\rho^*=0.4$ and $T^*=1.0$. Symbols show the simulated $C_v(t)$ and the full line represents the $C_v(t)$ obtained by MCT.

ties. As seen from the figures the theory is in good agreement with the simulation results both at short and long times. Nevertheless, the agreement is somewhat poorer in case of low density. This is expected since at low densities the friction itself develops a negative region, which slows down the decay of MCT $C_v(t)$. This negative region is not captured in the Gaussian approximation employed for bare friction ($\zeta(t)$). Hence, to get the better agreement at low densities one needs to add the t^4 term in the binary friction expression.

It is interesting to note that despite the existence of long time tails of $C_v(t)$, we can still have a well-defined diffusion coefficient. We find that the decay of the longitudinal current mode is sufficiently fast to preclude the existence of “dangerous” long time tails of VACF, thereby avoiding the divergence of diffusion in one dimension.

The agreement of the MCT results with the simulations supports our explanation that the long time t^{-3} decay of $C_v(t)$ arises from the coupling of the tagged particle’s motion with the longitudinal current mode of the surrounding fluid. To strengthen our argument we have also calculated the coefficient multiplying the t^{-3} tail, which is equal to 0.050 26 from the MCT and 0.065 97 from simulations. Given the uncertainties in the simulations and in the $g(x)$ which is also obtained from simulations, this agreement can be regarded as satisfactory.

For hard rods Lebowitz and Percus gave an exact expression for the diffusion coefficient,^{5,4}

$$D = \frac{(1-\rho l)}{\sqrt{(2\pi\beta m)\rho}}, \quad (23)$$

where l is the hard rod length. We find that such a relation for the density dependence holds good in case of LJ rods too. In Fig. 8 we have plotted the simulated D against $(1-\rho l)/\rho$. Symbols show the simulated D values and the straight line is the linear fit. From the figure we can see a clear linear dependence of D over the whole density range.

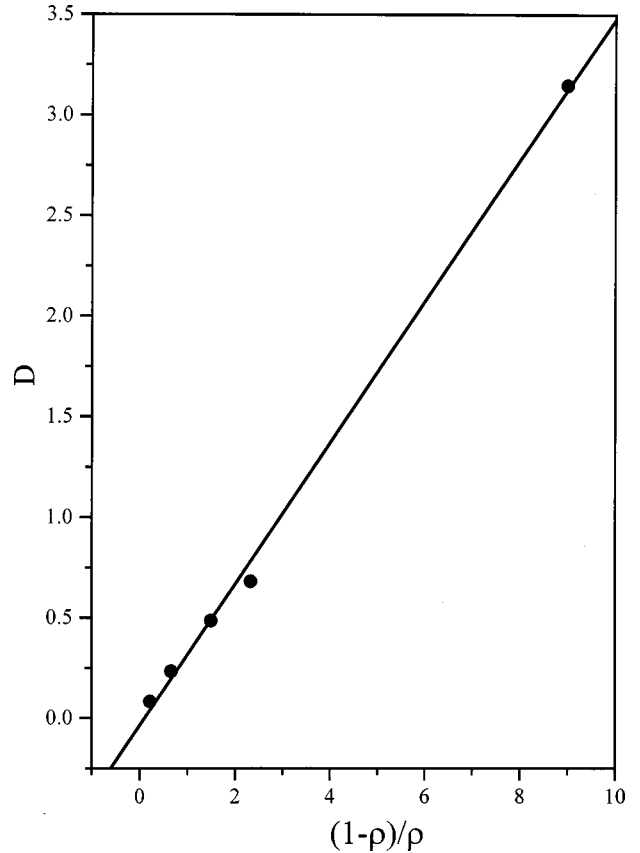


FIG. 8. Simulated diffusion coefficient is plotted against $(1-\rho l)/\rho$ at all the densities mentioned in Fig. 4. Symbols show the simulated D values and the straight line is the linear fit.

VI. CONCLUSION

We have carried out self-consistent mode coupling theory calculation and also molecular dynamic simulations to understand both the origin of the long time decay of $C_v(t)$ and also the density dependence of time dependent diffusion in the one dimensional Lennard-Jones system.

We found that in the low wave vector limit the dynamic structure factor is a Gaussian function of time. This intern gives rise to a t^{-3} decay of the longitudinal current correlation function. We have showed that the t^{-3} decay in velocity correlation arises from the coupling of the tagged particle’s motion to the longitudinal current mode of the fluid in the long time. We find that the decay of longitudinal current is sufficient faster to avoid any divergence in the diffusion. Even at high densities there exists a small but nonvanishing value of diffusion. We have observed that the existing exact solution for hard rods can be applied to LJ systems to describe the density dependence of diffusion over a wide density range.

ACKNOWLEDGMENTS

We thank S. Bhattacharyya, R. K. Murarka, and Dr. R. Aldrin Denny for helpful discussions. This work was supported in parts by grants from DST, India and CSIR, India. G.S. thanks CSIR, New Delhi, India, for a Research Fellowship.

¹Y. Pomeau and P. Resibois, Phys. Rep. **19**, 63 (1975).

²B. J. Alder and T. E. Wainwright, Phys. Rev. A **1**, 18 (1970).

³S. Bhattacharyya, G. Srinivas, and B. Bagchi, Phys. Lett. A **266**, 394 (2000).

⁴D. W. Jepsen, J. Math. Phys. **6**, 405 (1965).

⁵J. L. Lebowitz and J. K. Percus, Phys. Rev. **155**, 122 (1967); J. L. Lebowitz, J. K. Percus, and J. Sykes, *ibid.* **171**, 224 (1968).

⁶J. W. Haus and H. J. Raveche, J. Chem. Phys. **68**, 4969 (1978).

⁷M. Bishop, J. Chem. Phys. **75**, 4741 (1981).

⁸M. Bishop and B. J. Berne, J. Chem. Phys. **59**, 5337 (1973).

⁹T. Gaskell and S. Miller, J. Phys. C **11**, 3749 (1978).

¹⁰L. Sjogren and A. Sjolander, J. Phys. C **12**, 4369 (1979).

¹¹S. Bhattacharyya and B. Bagchi, Phys. Rev. E (in press).

¹²J. P. Hansen and I. R. McDonald, *Theory of Simple Liquids* (Academic, New York, 1986).

¹³S. Bhattacharyya, Ph.D. thesis, Indian Institute of Science, Bangalore, 1999.